Chemistry of NO_2 on Oxide Surfaces: Formation of NO_3 on $TiO_2(110)$ and NO_2↔O Vacancy Interactions

José A. Rodriguez,*,† Tomas Jirsak,† Gang Liu,† Jan Hrbek,† Joseph Dvorak,† and Amitesh Maiti‡

Contribution from the Department of Chemistry, Brookhaven National Laboratory, Upton, New York 11953, and Molecular Simulations Inc., 9685 Scranton Road, San Diego, California 92121

Received May 7, 2001

Abstract: Synchrotron-based high-resolution photoemission, X-ray absorption near-edge spectroscopy, and first-principles density functional (DF) slab calculations were used to study the interaction of NO_2 with a $TiO_2(110)$ single crystal and powders of titania. The main product of the adsorption of NO_2 on $TiO_2(110)$ is surface nitrate with a small amount of chemisorbed NO_2. A similar result is obtained after the reaction of NO_2 with polycrystalline powders of TiO_2 or other oxide powders. This trend, however, does not imply that the metal centers of the oxides are unreactive toward NO_2. An unexpected mechanism is seen for the formation of NO_3. Photoemission data and DF calculations indicate that the surface nitrate forms through the disproportionation of NO_2 on Ti sites ($2NO_{2,ads} \rightarrow NO_{3,ads} + NO_{gas}$) rather than direct adsorption of NO_2 on O centers of titania. Complex interactions take place between NO_2 and O vacancies of $TiO_2(110)$. Electronic states associated with O vacancies play a predominant role in the bonding and surface chemistry of NO_2. The adsorbed NO_2, on its part, affects the thermochemical stability of O vacancies, facilitating their migration from the bulk to the surface of titania. The behavior of the NO_2/titania system illustrates the importance of surface *and* subsurface defects when using an oxide for trapping or destroying NO_x species in the prevention of environmental pollution (DeNOx operations).

I. Introduction

Nitrogen oxides (NO_x), one of the most harmful environmental pollutants,[1] are formed in automotive engines and industrial combustion systems when air is used as an oxidant agent.[2] In the atmosphere, nitrogen oxides are a serious health hazard for the human respiratory system and contribute to the generation of smog and acid rain.[1] Although the elimination of nitrogen oxides from gas streams (DeNOx operations) has been a major concern for the past three decades, recently research in this area has intensified.[2−4] In part, this is motivated by the fact that there is evidence that emission of these noxious vapors into the atmosphere has increased.[4a,5] New and more stringent regulations on NO_x emissions emphasize the need for more efficient catalysts or sorbents for pollution control.[2]

NO_2 is produced in combustion processes under oxygen-rich conditions. Emerging technologies favor the formation of NO_2 instead of NO during the combustion of fuels because the higher reactivity of NO_2 makes easier subsequent DeNOx operations.[4b,6] NO_2 is a radical molecule,[7] with a large electron affinity (∼2.3 eV[8]), that can bond to metal centers via O, N, or a combination of both.[9] It is known that the chemistry of NO_2 on metal surfaces is rich.[10,11] The adsorbed molecule can undergo partial ($NO_2 \rightarrow NO + O$) or complete dissociation ($NO_2 \rightarrow N + 2O$), or disproportionate into NO_3 species ($2NO_2 \rightarrow NO_3 + NO$). Oxides can be very useful as sorbents or catalysts for trapping or destroying NO_2 and other NO_x species.[2−4] For example, oxides are used in NO_x storage technologies where the release of NO_2 at high temperatures is a key issue.[4c,12] In addition, oxides are able to catalyze the reduction of NO_2 by alkanes.[2,4b,6] However,

* Corresponding author. Fax: 631-344-5815. E-mail: rodrigez@bnl.gov.
† Brookhaven National Laboratory.
‡ Molecular Simulations Inc.

(1) Stern, A. C.; Boubel, R. W.; Turner, D. B.; Fox, D. L. *Fundamentals of Air Pollution*, 2nd ed.; Academic Press: Orlando, FL, 1984.

(2) (a) *Environmental Catalysis*; Armor, J. N., Ed.; ACS Symposium Series 552; American Chemical Society: Washington, DC, 1994. (b) Taylor, K. C. *Catal. Rev. Sci. Eng.* **1993**, *35*, 457. (c) Shelef, M.; McCabe, R. W. *Catal. Today* **2000**, *62*, 35.

(3) Thomas, J. M.; Thomas, W. J. *Principles and Practice of Heterogeneous Catalysis*; VCH: New York, 1997.

(4) (a) Belanger, R.; Moffat, J. B. *Appl. Catal. B* **1997**, *13*, 167. (b) Shimokawabe, M.; Itoh, K.; Takezawa, N. *Catal. Today* **1997**, *36*, 65. (c) Matsumoto, S.; Ikeda, Y.; Suzuki, H.; Ogai, M.; Miyoshi, N. *Appl. Catal. B* **2000**, *25*, 115. (d) Blanco, J.; Odenbrand, C.; Avila, P.; Knapp, C. *Catal. Today* **1998**, *45*, 103. (e) Matralis, H.; Theret, S.; Bastians, Ph.; Ruwet, M.; Grange, P. *Appl. Catal. B* **1995**, *5*, 271. (f) Kung, H. H.; Kung, M. C. *Catal. Today* **1996**, *30*, 5. (g) Ozkan, U. S.; Kumthekar, M. W.; Karakas, G. *Catal. Today* **1998**, *40*, 3. (h) Masaaki, H.; Kintaichi, Y.; Inaba, M.; Hideaki, H. *Catal. Today* **1998**, *42*, 127.

(5) (a) Lefohn, A. S.; Shadwick, D. S. *Atmos. Environ.* **1991**, *25A*, 491. (b) Tsai, S.; Bedell, S. A.; Kirby, L.; Zabcik, D. J. *Environ. Prog.* **1989**, *8*, 126.

(6) (a) Fischer, G. B., personal communication. (b) Shimokawabe, M.; Ohi, A.; Takezawa, N. *React. Kinet. Catal. Lett.* **1994**, *52*, 393. (c) Gutierrez, L.; Ribotta, A.; Boix, A.; Petunchi, J. *Stud. Surf. Sci. Catal.* **1996**, *101*, 631.

(7) Rodriguez, J. A. *Surf. Sci.* **1990**, *230*, 335.

(8) (a) Hughes, B. M.; Lifshitz, C.; Tiernan, T. O. *J. Chem. Phys.* **1973**, *59*, 3162. (b) Herbst, E.; Patterson, T. A.; Lineberger, W. C. *J. Chem. Phys.* **1974**, *61*, 1300.

(9) Hitchman, M. A.; Rowbottom, G. L. *Coord. Chem. Rev.* **1982**, *42*, 55.

(10) Jirsak, T.; Kuhn, M.; Rodriguez, J. A. *Surf. Sci.* **2000**, *457*, 254 and references therein.

(11) (a) Outka, D. A.; Madix, R. J.; Fischer, G. B.; Di Maggio, C. *Surf. Sci.* **1987**, *179*, 1. (b) Schwalke, U.; Parmeter, J. E.; Weinberg, W. H. *J. Chem. Phys.* **1986**, *84*, 4036. (c) Hrbek, J.; van Campen, D. G.; Malik, I. J. *J. Vac. Sci. Technol. A*, **1995**, *13*, 1409. (d) Bartram, M. E.; Windham, R. G.; Koel, B. E. *Surf. Sci.* **1987**, *184*, 57.

(12) Schneider, W. F.; Hass, K. C., personal communication.

10.1021/ja011131i CCC: $20.00 © 2001 American Chemical Society
Published on Web 09/07/2001

very little is known about the basic chemistry of NO_2 on oxide surfaces.[13] A few surface science studies have been carried out on epitaxial oxide films (Cr_2O_3,[14,15] MgO,[16] CeO_2,[16,17] $Ce_{0.8}Zr_{0.2}O_2$[17]) grown on metal or oxide supports, and on a ZnO(0001)−Zn single crystal.[18] There is a clear need to obtain a more complete understanding of the bonding and behavior of NO_2 on oxides.[6,12,13]

Titania is an important component in NO_x storage−reduction catalysts.[4c−h] In the present work, we use synchrotron-based high-resolution photoemission, X-ray absorption near-edge spectroscopy (XANES), and first-principles density-functional (DF) slab calculations to study the interaction of NO_2 with a TiO_2(110) single crystal and powders of titania. The (110) face of TiO_2 in the rutile crystal structure is interesting because it exposes metal and oxygen atoms, allowing a direct comparison of the reactivity of these adsorption sites. Our results show an unexpected mechanism for the formation of NO_3 on titania. A very important issue in oxide catalysis is the role of surface defects in determining the activity and selectivity of the catalyst.[19,20] It is well known how to generate O vacancies in the TiO_2(110) substrate.[13,21] Combining experiments and theoretical calculations, we examined in detail the bonding of NO_2 to vacancy structures on the oxide surface. The presence of O vacancies leads to complex interactions in the NO_2/TiO_2(110) system. On one hand, O vacancies induce new electronic states in the oxide that favor the adsorption of NO_2 and drastically alter the surface chemistry of this molecule. On the other hand, the adsorbed NO_2 substantially affects the thermochemical stability of the O vacancies in the surface. Our results clearly show that NO_x species induce the migration of O vacancies from the bulk toward the surface of an oxide. These phenomena can control the efficiency of an oxide as a sorbent or catalyst in DeNOx operations.

II. Experimental and Theoretical Methods

II.1. Photoemission Experiments. The photoemission experiments for the adsorption of NO_2 on the (110) face of TiO_2 in the rutile crystal structure were performed in a standard ultra-high-vacuum (UHV) chamber (base pressure $\sim 6 \times 10^{-10}$ Torr) that is part of the U7A beamline of the National Synchrotron Light Source (NSLS) at Brookhaven National Laboratory.[16,17,22] This UHV chamber contains a hemispherical electron energy analyzer with multichannel detection, instrumentation for low-energy electron diffraction (LEED), a quadrupole mass spectrometer, and a dual-anode Mg/Al Kα source. The N 1s and valence spectra were taken using a photon energy of 500 eV, whereas a photon energy of 625 eV was used to collect the Ti 2p and O 1s data. The binding energy scale of the photoemission spectra was calibrated by the position of the Fermi edge.[22] The overall instrumental resolution in the photoemission experiments was ~0.35 eV.

Mounting of the TiO_2(110) sample in the UHV chamber was done according to the procedure described in ref 23. In short, the oxide sample was sandwiched between Ta plates that were spot-welded to two Ta heating legs of a manipulator capable of cooling to 80 K and heating to 1100 K. The TiO_2(110) crystal was cleaned by ion bombardment with 1 keV Ne^+ ions at room temperature, followed by annealing in UHV for 10 min at 970 K.[21,22] This sample treatment produced a (1 × 1) LEED pattern, and previous studies using scanning tunneling microscopy[21] and photoemission[23] have shown that the resulting surface has O vacancies with a density of ~7%. NO_2 was dosed to the TiO_2(110) surface through a glass-capillary array doser[16−18] positioned to face the sample at a distance of ~2 mm. The NO_2 exposures are based on the ion gauge reading and were not corrected for the capillary array enhancement.

II.2. XANES Experiments. Powders of the rutile and anatase phases of TiO_2 plus other oxides (MgO, CeO_2, Cr_2O_3, Fe_2O_3, CuO, ZnO) were exposed to NO_2 in an RXM-100 instrument from Advanced Scientific Designs. This was done in a reaction cell (batch-reactor mode) at 300 K for 15 min with constant gas pressures of 400−500 Torr. All the oxide powders were obtained from commercial sources and had a purity in excess of 99%. The oxides were cleaned before exposure to NO_2 by heating (400−700 K) in a vacuum or in the presence of O_2 until they displayed typical O K-edge XANES and core-level photoemission spectra.[18,20e] Beamline U7A of the NSLS was used to collect the N and O K-edge XANES data. These spectra were taken in the electron-yield mode by using a channeltron multiplier located near the sample surface. The energy resolution was close to 0.3 eV.

II.3. Theoretical Methods and Models. The first-principles density functional (DF) calculations reported in section III were performed using the commercial version of the CASTEP code[24] available from Molecular Simulations Inc. CASTEP has an excellent track record in accurate prediction of geometry and energetics for oxide systems.[15,16,22,24−28] In this code, the wave functions of valence electrons are expanded in a plane wave basis set with *k*-vectors within a specified energy cutoff E_{cut}. Tightly bound core electrons are represented by nonlocal ultrasoft pseudopotentials.[29] Brillouin zone integration is approximated by a sum over special *k*-points chosen using the Monkhorst−Pack scheme.[30] The exchange-correlation contribution to the total electronic energy is treated in a spin-polarized generalized-gradient corrected (GGA) form of the local density approximation (LDA).[31] In all the calculations, the kinetic energy cutoff E_{cut} and the density of the Monkhorst−Pack *k*-point mesh were chosen high enough to ensure convergence of the computed structures and energetics. Since the DF calculations were performed at the GGA level, one can expect good predictions for the bonding energies of the NO_2 molecule on TiO_2.[31,32] For the interaction of NO with oxides, DF-GGA calculations predict adsorption energies within an accuracy of 5 kcal/mol.[25a,33] In any case, in this work our main interest is in qualitative trends in the energetics, and not in absolute values. For each

(13) Henrich, V. E.; Cox, P. A. *The Surface Science of Metal Oxides*; Cambridge University Press: Cambridge, U.K., 1994.
(14) Xu, C.; Hassel, M.; Kuhlenbeck, H.; Freund, H.-J. *Surf. Sci.* **1991**, *258*, 23.
(15) Rodriguez, J. A.; Pérez, M.; Jirsak, T.; González, L.; Maiti, A.; Larese, J. Z. *J. Phys. Chem. B* **2001**, *105*, 5497.
(16) Rodriguez, J. A.; Jirsak, T.; Sambasivan, S.; Fischer, D.; Maiti, A. *J. Chem. Phys.* **2000**, *112*, 9929.
(17) Liu, G.; Rodriguez, J. A.; Hrbek, J.; Dvorak, J.; Peden, C. H. F. *J. Phys. Chem. B* **2001**, *105*, 7762.
(18) Rodriguez, J. A.; Jirsak, T.; Chaturvedi, S.; Dvorak, J. *J. Mol. Catal. A: Chemical* **2001**, *167*, 47.
(19) Chen, M.; Friend, C. M.; Kaxiras, E. *J. Am. Chem. Soc.* **2001**, *123*, 2224 and references therein.
(20) (a) Kung, H. H. *Transition Metal Oxides: Surface Chemistry and Catalysis*; Elsevier: New York, 1989. (b) Freund, H.-J. *Faraday Discuss.* **1999**, *114*, 1. (c) Campbell, C. T. *Surf. Sci. Rep.* **1997**, *27*, 1. (d) Street, S. C.; Xu, C.; Goodman, D. W. *Annu. Rev. Phys. Chem.* **1997**, *48*, 43. Chen, J. G. *Surf. Sci. Rep.* **1997**, *30*, 1.
(21) Hebenstreit, E. L. D.; Hebenstreit, W.; Diebold, U. *Surf. Sci.* **2000**, *461*, 87.
(22) Rodriguez, J. A.; Hrbek, J.; Dvorak, J.; Jirsak, T.; Maiti, A. *Chem. Phys. Lett.* **2001**, *336*, 377.
(23) Hrbek, J.; Rodriguez, J. A.; Dvorak, J.; Jirsak, T. *Collect. Czech. Chem. Commun.*, in press.
(24) (a) Payne, M. C.; Allan, D. C.; Arias, T. A.; Johannopoulus, J. D. *Rev. Mod. Phys.* **1992**, *64*, 1045. (b) Milman, V.; Winkler, B.; White, J. A.; Pickard, C. J.; Payne, M. C.; Akhmatskaya, E. V.; Nobes, R. H. *Int. J. Quantum Chem.* **2000**, *77*, 895.
(25) (a) Sorescu, D. C.; Rusu, C. N.; Yates, J. T. *J. Phys. Chem. B* **2000**, *104*, 4408. (b) Sorescu, D. C.; Yates, J. T. *J. Phys. Chem. B* **1998**, *102*, 4556.
(26) Rodriguez, J. A.; Maiti, A. *J. Phys. Chem. B* **2000**, *104*, 3630.
(27) Refson, K.; Wogelius, R. A.; Fraser, D. G.; Payne, M. C.; Lee, M. H.; Milman, V. *Phys. Rev. B* **1995**, *52*, 10823.
(28) (a) Rodriguez, J. A.; Jirsak, T.; Pérez, M.; Chaturvedi, S.; Kuhn, M.; González, L.; Maiti, A. *J. Am. Chem. Soc.* **2000**, *122*, 12362. (b) Rodriguez, J. A.; Pérez, M.; Jirsak, T.; González, L.; Maiti, A. *Surf. Sci.* **2001**, *477*, L279.
(29) Vanderbilt, D. *Phys. Rev. B* **1990**, *41*, 7892.
(30) Monkhorst, H. J.; Pack, J. D. *Phys. Rev. B* **1976**, *13*, 5188.
(31) White, J. A.; Bird, D. M. *Phys. Rev. B* **1994**, *50*, 4954.
(32) (a) Ziegler, T. *Chem. Rev.* **1991**, *91*, 651. (b) van Santen, R. A.; Neurock, M. *Catal. Rev.-Sci. Eng.* **1995**, *37*, 557. Rodriguez, J. A. *Theor. Chem. Acc.*, submitted.
(33) Rodriguez, J. A.; Jirsak, T.; Pérez, M.; González, L.; Maiti, A. *J. Chem. Phys.* **2001**, *114*, 4186.

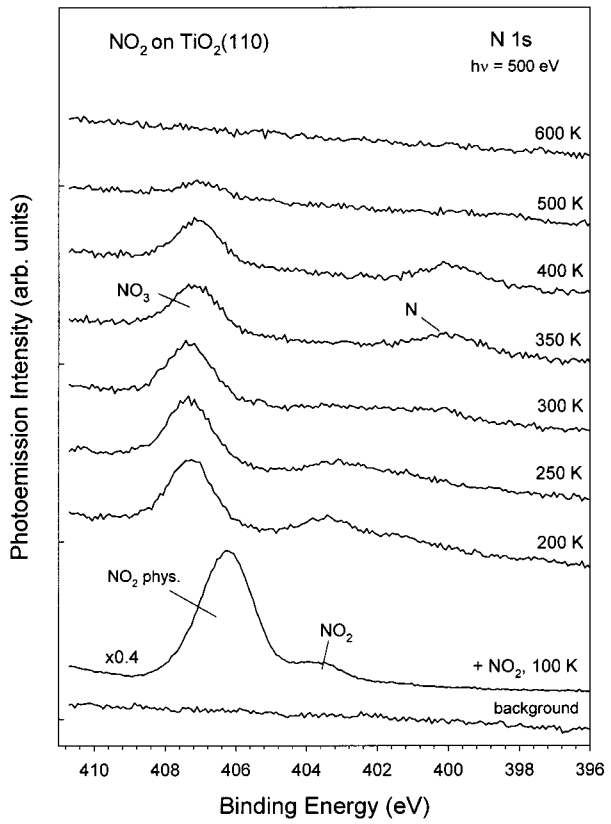

Figure 1. N 1s spectra acquired after depositing a multilayer of NO_2 on $TiO_2(110)$ at 100 K, with subsequent heating to higher temperatures. The electrons were excited using a photon energy of 500 eV.

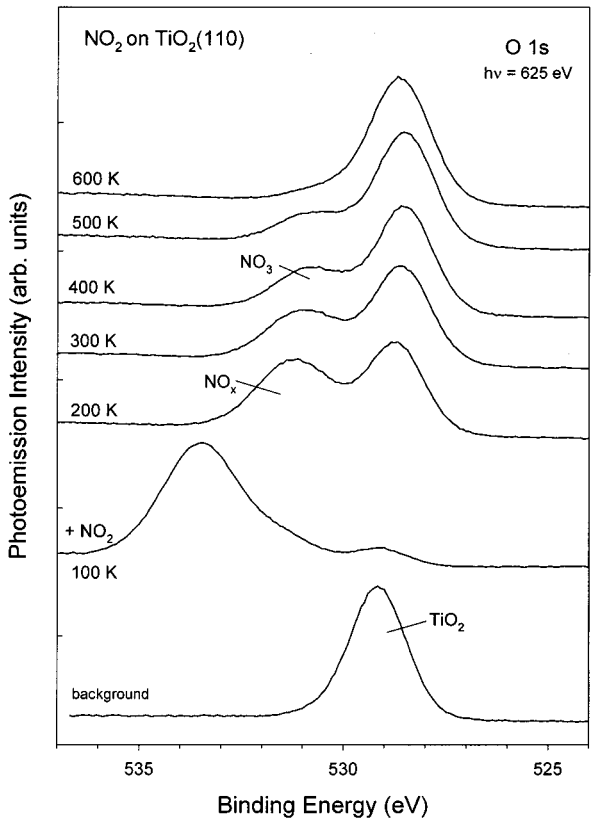

Figure 2. O 1s spectra taken after adsorbing a multilayer of NO_2 on $TiO_2(110)$ at 100 K, with subsequent heating to higher temperatures. A photon energy of 625 eV was used to take these spectra.

optimized structure, the partial charges on the atoms were estimated by projecting the occupied one-electron eigenstates onto a localized basis set with a subsequent Mulliken population analysis.[34,35] Mulliken charges have well-known limitations[36] but are nevertheless useful as a qualitative tool.

III. Results

III.1. Reaction of NO_2 with TiO_2. Figure 1 shows N 1s photoemission spectra acquired after depositing a multilayer of NO_2 on a $TiO_2(110)$ surface at 100 K with subsequent annealing to higher temperatures. Upon dosing of nitrogen dioxide at 100 K, two clear features are observed. The peak near 403.5 eV corresponds to chemisorbed NO_2,[16] whereas the peak at ~406 eV can be assigned to physisorbed NO_2 (or N_2O_4 dimers[11b]) since it disappeared after heating above 150 K.[17,18] For small and medium exposures of NO_2 gas (not shown), only the N 1s signal of chemisorbed NO_2 was detected at 100 K. By 200 K, the intensity of the peak for chemisorbed NO_2 in Figure 1 has decreased, and a new strong peak is seen at ~407 eV that matches the binding energy position reported for chemisorbed NO_3.[16,18] Following a common line of thought,[37] one could assume that the nitrate is formed by direct interaction of NO_2 with O atoms of the oxide surface:

$$NO_2(\text{gas or ads}) + O(\text{surface}) \rightarrow NO_3(\text{ads}) \qquad (1)$$

But, if this is the case, *it is difficult to understand why NO_2 is bonded to Ti sites at 100 K instead of reacting with O to form the more stable NO_3 species*. The validity of this hypothesis will be tested by means of DF calculations in section III.2. In Figure 1, heating to 300 K removes the signal for NO_2, and features for atomic nitrogen begin to appear near 399 eV.[16,18] From 300 to 400 K, there is a decrease in the signal for NO_3 and an increase in the signal for N. Around 500 K, only a small amount of NO_3 is seen on the surface, which completely disappears upon final heating to 600 K.

O 1s spectra for the adsorption of NO_2 on $TiO_2(110)$ are shown in Figure 2. The clean oxide exhibits a peak near 529.2 eV. This peak is almost completely attenuated after deposition of a multilayer of NO_2 on the surface at 100 K. The physisorbed NO_2 desorbs upon heating to 200 K, leaving an O 1s spectrum with peaks for TiO_2 (~528.7 eV) and chemisorbed NO_x species (~531.3 eV). The binding energy shift in the position of the TiO_2 features (~0.5 eV) could be a result of changes in band bending[20c] induced by the adsorbates (NO_3 and NO_2, see Figure 1). Heating from 200 to 400 K causes desorption of NO_2 from the surface, and there is a shift and decrease in the intensity of the NO_x features in Figure 2. These features are completely removed upon heating to 600 K. The photoemission results in Figures 1 and 2 indicate that NO_2 reacts with a $TiO_2(110)$ surface to form stable NO_3 species with relatively minor amounts of NO_2 and N.

Polycrystalline powders of TiO_2 (rutile or anatase structures) were exposed to a moderate pressure of NO_2 (~450 Torr) at 300 K. Figure 3 displays typical XANES data at the N K-edge for these systems and two common standards (KNO_2, KNO_3) which show the electronic transitions within the NO_3 and NO_2

(34) Segall, M. D.; Pickard, C. J.; Shah, R.; Payne, M. C. *Phys. Rev. B* **1996**, *54*, 16317.
(35) Segall, M. D.; Pickard, C. J.; Shah, R.; Payne, M. C. *Mol. Phys.* **1996**, *89*, 571.
(36) (a) Szabo, A.; Ostlund, N. S. *Modern Quantum Chemistry*; McGraw-Hill: New York, 1989. (b) Wiberg, K. B.; Rablen, P. R. *J. Comput. Chem.* **1993**, *14*, 1504.
(37) Dines, T. J.; Rochester, C. H.; Ward, A. M. *J. Chem. Soc., Faraday Trans.* **1991**, *87*, 643 and references therein.

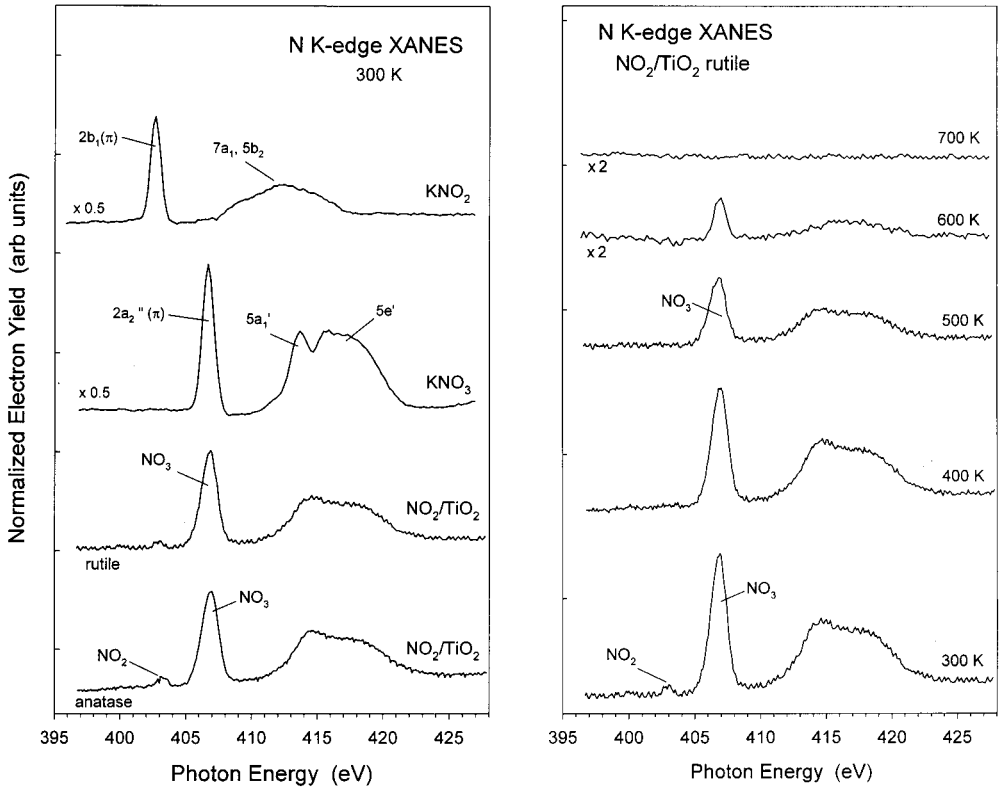

Figure 3. (Left) N K-edge XANES results for TiO_2 powders (anatase or rutile structures) exposed to NO_2 at 300 K. For comparison, we also include the results for two common standards: KNO_2 and KNO_3. (Right) N K-edge spectra taken after exposing a powder of TiO_2 (rutile structure) to NO_2 (450 Torr, 15 min) at 300 K, followed by evacuation of the gas and heating in a vacuum to 400, 500, 600, and 700 K.

groups. In the spectrum for the pure nitrate, the intense resonance at a photon energy of ~407 eV corresponds to 1s → $2a_2''(\pi)$ electronic transitions, whereas the broad features between 410 and 420 eV probably come from excitations into the $5a_1'$ and $5e'$ empty σ orbitals of NO_3.[7] In the case of the NO_2 salt, the first strong peak at ~403 eV corresponds to 1s → $2b_1(\pi)$ electronic transitions, with the envelope from 407 to 417 eV probably resulting from excitations into $7a_1$ and $5b_2$ vacant σ orbitals of nitrogen dioxide.[7] In Figure 3, the spectra for the TiO_2 powders exposed to nitrogen dioxide show strong resonances for NO_3 and a weak signal for NO_2. Heating to higher temperatures led to removal of the features for chemisorbed NO_2 by 400 K, and NO_3 by 700 K. This is similar to the trends seen after adsorbing NO_2 on the $TiO_2(110)$ surface. Since polycrystalline powders of TiO_2 expose a substantial amount of Ti centers on their surfaces,[13,20a] the lack of a strong signal for chemisorbed NO_2 in Figure 3 could be attributed[37] to a low reactivity of the Ti centers with NO_3 being formed by the interaction of NO_2 with O centers, reaction 1. A different interpretation will be presented below.

III.2. Bonding of NO_2 to $TiO_2(110)$ and Formation of NO_3. The bonding of NO_2 to the (110) face of titania in a rutile structure was studied using DF-GGA calculations. The TiO_2-(110) surface was represented by a four-layer slab as shown in Figure 4, which was embedded in a three-dimensionally periodic supercell.[22,24,25] A vacuum of 12 Å was placed on top of the slab in order to ensure negligible interactions between periodic images normal to the surface.[22,24,27] Previous theoretical studies have shown that a three-layer periodic slab can reliably model adsorption reactions on a perfect $TiO_2(110)$ surface.[22,25,38] In our calculations, we added one more layer since we are also interested in examining the behavior of titania systems with vacancies on the surface and subsurface region (section III.4). The geometry optimization for bulk TiO_2 gave a rutile unit cell with $a = b = 4.64$ Å and $c = 2.97$ Å. These values are close to those derived from experimental measurements ($a = b =$ 4.59 Å, $c = 2.96$ Å)[39] and other theoretical calculations.[25,38b] In the slab calculations, the structural geometry of the first two layers was relaxed, while the other two layers were kept fixed in the geometry of bulk TiO_2. For the perfect $TiO_2(110)$ surface, the 5-fold- and 6-fold-coordinated Ti ions moved in and out of plane by 0.15 and 0.11 Å, respectively. The bridging oxygens moved into the surface by 0.10 Å, and the in-plane oxygens moved out of the surface by 0.11 Å. These shifts in the atom positions agree well with those seen in other DF studies.[25,38b] Most of them are also in good agreement with atomic shifts found in X-ray surface diffraction studies for $TiO_2(110)$,[40] the only exception being the shift for the bridging oxygens, where the experimental results give a movement of 0.27 Å toward the surface.

Before studying the adsorption of NO_2 on $TiO_2(110)$, we examined the adsorption of NO as a test case. The NO molecule ($\theta_{NO} = 0.25$ ML) was bonded to atoms in the bridging O rows (via N) or atoms in the Ti rows (via N or O). In agreement with previous infrared and DF-GGA studies,[25a,41] we found that bonding to Ti via N was the most stable configuration. The calculated NO adsorption energy (11.6 kcal/mol) was close to

(38) (a) Pacchioni, G.; Ferrari, A. M.; Bagus, P. S. *Surf. Sci.* **1996**, *350*, 159. (b) Albaret, T.; Finocchi, F.; Noguera, C. *Faraday Discuss.* **1999**, *114*, 285. (c) Yang, Z.; Wu, R.; Zhang, Q.; Goodman, D. W. *Phys. Rev. B* **2001**, *63*, 045419.

(39) Abrahams, S. C.; Bernstein, J. L. *J. Chem. Phys.* **1971**, *55*, 3206.

(40) Charlton, G.; Howes, P. B.; Nicklin, C. L.; Steadman, P.; Taylor, J. S. G.; Muryn, C. A.; Harte, S. P.; Mercer, J.; MacGrath, R.; Norman, D.; Turner, T. S.; Thorton, G. *Phys. Rev. Lett.* **1997**, *78*, 495 and references therein.

(41) Rusu, C. N.; Yates, J. T. *J. Phys. Chem. B* **2000**, *104*, 1729.

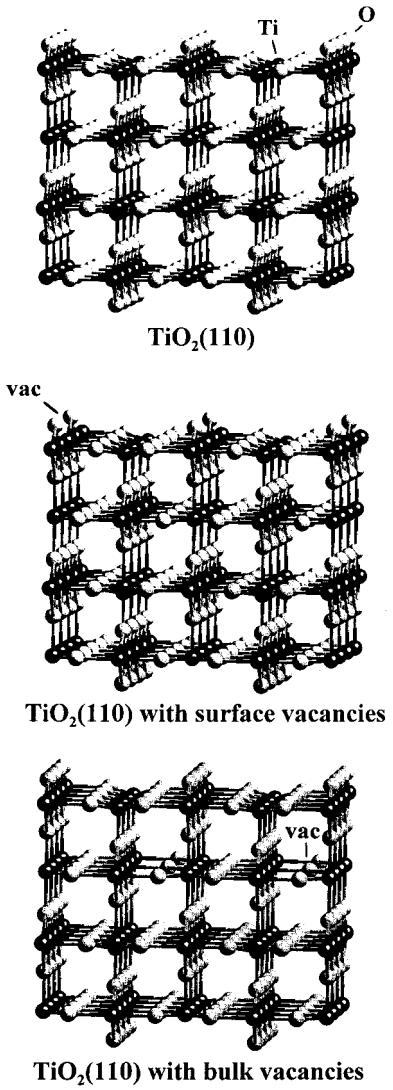

Figure 4. Slabs used to model a perfect TiO_2(110) surface, and systems with O vacancies in the surface (center) or subsurface (bottom) regions. Each slab contains four layers with Ti atoms. Ti atoms are represented by dark spheres, whereas gray spheres correspond to O atoms.

that determined from thermal desorption measurements (8.4 kcal/mol[25a]).

Nitrogen dioxide was adsorbed on oxygen and metal centers of TiO_2(110) in the bonding configurations shown in Figure 5. The adsorption of NO_2 on atoms of the bridging O rows (η^1-N on O, in our notation) produces NO_3-like species in accordance with reaction 1. On Ti sites, NO_2 can bond via nitrogen (η^1-N) or the oxygens (η^2-O,O). Both bonding configurations have been observed on transition metal surfaces.[7,10,11] Table 1 displays adsorption geometries and bonding energies predicted by CASTEP for a NO_2 coverage of 0.25 ML on TiO_2(110). In our DF-GGA calculations, the geometries of the adsorbate and two slab layers near the surface were optimized. In contrast to the case of adsorbed NO, where bonding to Ti through the N end has been observed,[25a,41] NO_2 prefers to bond to the oxide cations via the oxygens. An identical difference is found when comparing the forms of bonding of NO and NO_2 on metal surfaces.[10,42] On Ti centers of TiO_2(110), NO_2 interacts more strongly than NO, with the electron density on adsorbed NO_2 ($q \approx -0.13$e) being larger than that on adsorbed NO ($q \approx +0.06$e). In the gas phase, NO and NO_2 have low-lying half-occupied electron-

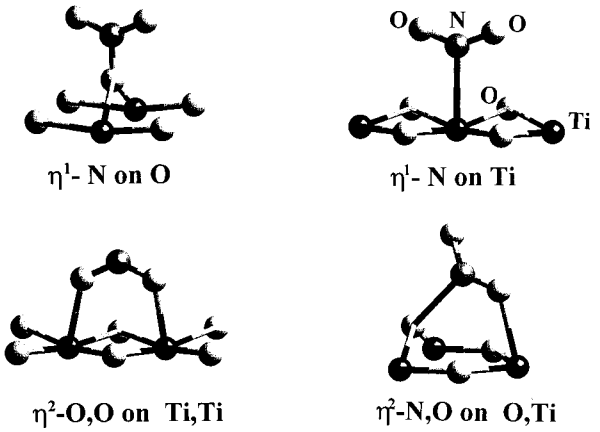

Figure 5. Bonding geometries for NO_2 on a perfect TiO_2(110) surface. Ti atoms are represented by dark spheres, whereas gray spheres correspond to O atoms.

Table 1. Adsorption of NO_2 on TiO_2(110): DF-GGA Results

	bond lengths (Å)				NO_2 charge, q (electrons)	ads energy (kcal/mol)[b]
	Ti−N	Ti−O	Os−N[a]	N−O		
free NO_2				1.21		
on Ti sites[c]						
η^1-N on Ti	2.67			1.22	−0.04	13.4
η^2-O,O on Ti,Ti		2.29		1.25	−0.18	21.3
on O sites[c]						
η^1-N on O			1.39	1.22	−0.03	15.1

[a] "Os" refers to an atom in the bridging O rows. [b] Positive values denote an exothermic process.[22,26] [c] $\theta_{NO_2} = 0.25$ ML.

acceptor orbitals:[43,44] 2π in NO, and $6a_1$ in NO_2. The relative energy positions of the NO(2π) and NO_2($6a_1$) orbitals[43,44] indicate that the dioxide should be the better electron acceptor and the more reactive species on TiO_2, in agreement with the trends seen in the DF calculations. In Table 1, *it is clear that the bonding interactions of NO_2 with two Ti atoms are stronger than with O*. Atoms in the bridging O rows of TiO_2(110) do not make strong bonds with NO_2, and the calculated adsorption energy (∼15 kcal/mol) on these sites is not consistent with the large thermal stability observed for the nitrate species in the experimental results of Figure 1. As an alternative to reaction 1, we must find other viable route(s) for the formation of NO_3 on a TiO_2(110) surface.

A variant of reaction 1 involves the abstraction of bridging O from the oxide by NO_2 (adsorbed in a η^2-O,O configuration) to form a bidentate nitrate species on the Ti sites. We calculated that this process is ∼36 kcal/mol *uphill* with respect to η^2-O,O chemisorbed NO_2 and, thus, can be ruled out as a route for obtaining a stable NO_3 species. Another possible pathway for the formation of NO_3 could be the adsorption of NO_2 in an η^2-N,O configuration on O and Ti centers (see bottom of Figure 5). In this case, the calculated adsorption energy (18.4 kcal/mol) is comparable to that seen for an η^2-O,O conformation on two Ti sites (21.3 kcal/mol), but not large enough to account for the high temperatures observed in Figure 1 for the decomposition of NO_3. Finally, NO_3 could be formed as a result

(42) Brown, W. A.; King, D. A. *J. Phys. Chem. B* **2000**, *104*, 2578.

(43) Rodriguez, J. A.; Jirsak, T.; Kim, J.-Y.; Larese, J. Z.; Maiti, A. *Chem. Phys. Lett.* **2000**, *330*, 475.

(44) (a) In the gas phase, NO and NO_2 are radical molecules with a low-lying half-occupied electron-acceptor orbital. The half-occupied orbital of NO_2, the $6a_1$ orbital, is ∼2 eV more stable than the half-occupied orbital of NO, the 2π orbital.[15,43] The experimental electron affinity of NO_2 is 1.7 eV larger than that of free NO.[44b,c] (b) Refaey, K. M. A. *Int. J. Mass Spectrom. Ion Phys.* **1976**, *21*, 21. (c) Leffert, C. B.; Jackson, W. M.; Rothe, E. W. *J. Chem. Phys.* **1973**, *58*, 5801.

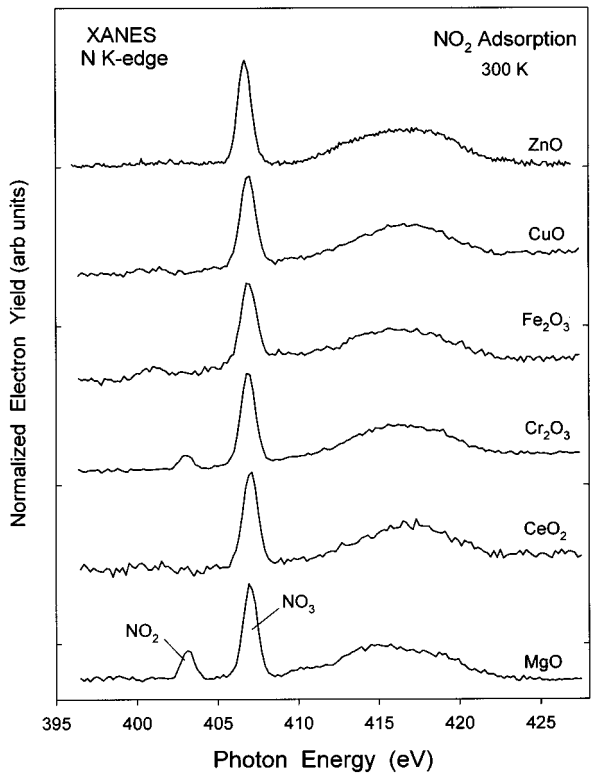

Figure 6. N K-edge XANES spectra taken after exposing powders of MgO, CeO_2, Cr_2O_3, Fe_2O_3, CuO, and ZnO to NO_2 (~450 Torr, 15 min) at 300 K.

of the disproportionation of NO_2 on Ti sites:

$$2NO_2(ads) \rightarrow NO_3(ads) + NO(gas) \qquad (2)$$

We calculated an energy change of −8 kcal/mol (exothermic process) for this reaction when the formed NO_3 is bidentate on Ti sites (η^2-O,O bonding) and has a coverage of 0.25 ML. To decompose the produced nitrate

$$NO_3(ads) \rightarrow O(ads) + NO_2(gas) \qquad (3)$$

one has to put 41 kcal/mol of energy into the system. This value is consistent with the elevated temperatures seen experimentally for the decomposition of NO_3 on TiO_2(110).

The theoretical results described in this section show that the Ti↔NO₂ interactions on TiO₂(110) are strong, and as a result of them the cations can get covered with nitrate. This unexpected mechanism for NO_3 formation is consistent with the photoemission data in Figure 1, where chemisorbed NO_2 is present at 100 K and its signal decreases upon heating to 200 K with simultaneous appearance of NO_3. In addition, reaction 2 explains the lack of an intense signal for chemisorbed NO_2 in the N K-edge XANES spectra of Figure 3. The metal centers exposed on the surfaces of polycrystalline powders of TiO_2 are more reactive than those in a TiO_2(110) surface, and upon interaction with NO_2 probably react fast, forming NO_3 groups. Reaction 2 must be taken into consideration when using oxides in DeNOx operations. Figure 6 shows XANES spectra for the adsorption of NO_2 on a series of polycrystalline powders. All these oxides contain metal centers in their surfaces,[13,20a] and the weak or missing signal for chemisorbed NO_2 does not imply a lack of reactivity of these metal centers toward NO_2. Such a behavior will not be compatible with the fact that the metal centers in these oxides interact well with molecules that are less chemically active than NO_2.[13,20] It is much more likely that

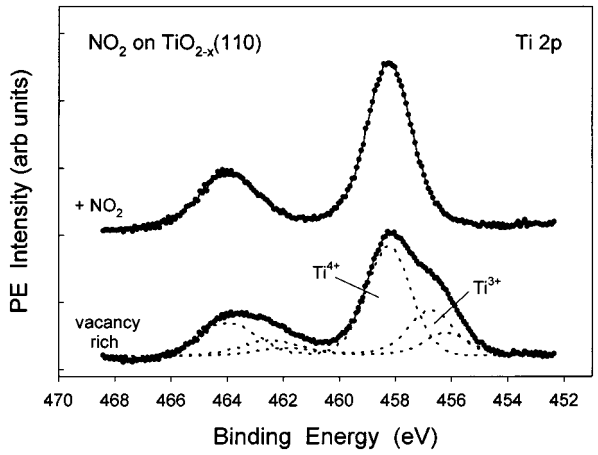

Figure 7. Ti 2p spectra taken before and after adsorbing NO_2 on an O-vacancy-rich TiO_{2-x}(110) surface at 300 K. The spectrum for the clean TiO_{2-x}(110) surface at the bottom was curve-fitted using a convolution of Gaussian and Lorentzian functions.[22,23] A photon energy of 625 eV was used to acquire these spectra.

in all these oxide systems the surface metal centers get covered with nitrate upon exposure to NO_2. Support for this idea is provided by the experiments in the following section for NO_2 on O-vacancy-rich titania.

III.3. Reaction of NO_2 with Defect-Rich TiO_{2-x}(110). In general, an important issue in oxide catalysis is the role of surface defects in determining the activity and selectivity of the catalyst.[19,20,25a,43,45] It is well known how to generate O vacancies in the TiO_2(110) substrate.[13,21,46] These O vacancies are distributed from the surface to the bulk of the material and lead to Ti centers with relatively low formal oxidation states (≤3+). We found that NO_2 is very efficient for the reoxidation of these Ti centers. The type of oxide surface used in the experiments of Figures 1 and 2 contains O vacancies with a density of ~7%.[21,23] For these systems, the associated Ti^{3+} centers completely transform into Ti^{4+} upon reaction with NO_2 at 300 K. A more extreme case is shown in Figure 7. A titania system rich in O vacancies and defects was produced by Ne^+ bombardment and subsequent annealing at 950 K. The resulting Ti 2p spectrum (bottom of Figure 7) exhibited very broad features. Curve-fitting indicates that the complex Ti 2p features arise from the convolution of three doublets, which correspond to Ti^{4+}, Ti^{3+}, and a Ti species in an even lower oxidation state ($Ti^{\delta+}$, $\delta < 3$). After a dose of 10 L of NO_2 at 300 K, only a well-defined doublet for Ti^{4+} was observed. The adsorbate *was able to eliminate all the Ti^{3+} and $Ti^{\delta+}$ sites in the surface and subsurface region* probed by photoemission (2−3 layers). Since NO_2 is a bulky molecule, this result implies that O vacancies and related defects migrate toward the oxide surface in the presence of NO_2. This interesting phenomenon will be studied in more detail in section III.4 using DF calculations.

Oxygen vacancies drastically change the chemistry of NO_2 on a titania surface. Figure 8 displays N 1s spectra taken after dosing NO_2 at 300 K to a TiO_{2-x}(110) system characterized by broad Ti 2p features such as those seen in Figure 7. Initially this defect-rich system is very reactive, and for the first dose of NO_2 a clear peak is observed near 399 eV for atomic N[43] produced by full decomposition of the adsorbate:

$$NO_2(gas) \rightarrow N(ads) + 2O(ads) \qquad (4)$$

(45) Kolmakov, A.; Stultz, J.; Goodman, D. W. *J. Chem. Phys.* **2000**, *113*, 7564.

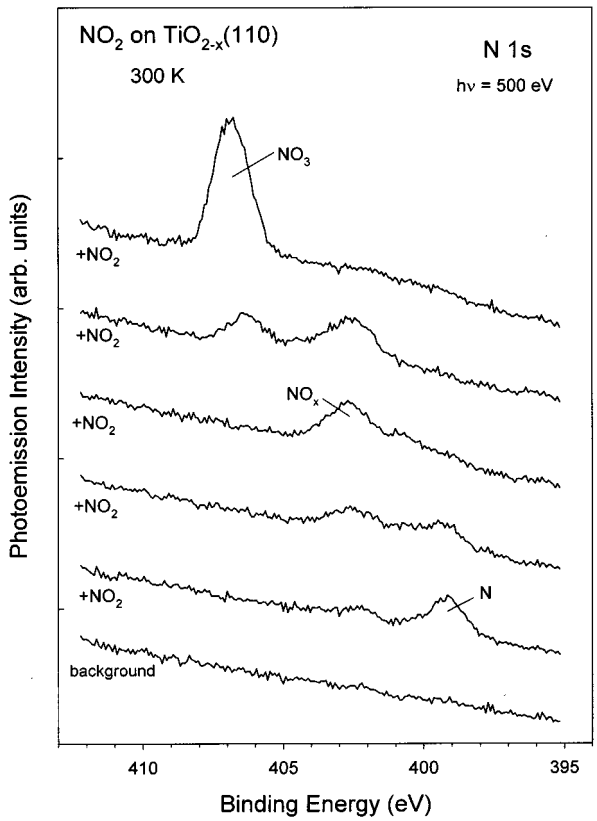

Figure 8. N 1s spectra acquired after several doses of NO_2 (0.2, 0.5, 1.0, 2.0, and 5.0 L) to an O-vacancy-rich $TiO_{2-x}(110)$ surface at 300 K. The electrons were excited using a photon energy of 500 eV.

The features for atomic N disappear upon additional dosing of NO_2, probably due to oxidation of the surface by the reaction:

$$NO_2(gas) \rightarrow NO(gas) + O(ads) \quad (5a)$$

$$nO(ads) + N(ads) \rightarrow NO_x(ads) \quad (5b)$$

Reaction 5a is known to be very effective for the oxidation of metals.[10,11c] The fact that oxides are more stable than nitrides[47] favors the replacement of Ti−N bonds with Ti−O bonds. At medium size doses of NO_2, a peak is seen at ∼402.5 eV in Figure 8. Such position is between those expected for chemisorbed NO (401−402 eV) and NO_2 (403−404 eV).[15,16,43] At the end, after a big dose of NO_2, there is a large content of oxygen in the system (i.e., the oxygen vacancies have been eliminated), and only NO_3 is observed on the surface. The same product was found for the interaction of NO_2 with a $TiO_2(110)$ surface (see Figure 1). The photoemission results in Figures 7 and 8 give a good indication of what may happen when polycrystalline powders of oxides are exposed to moderate pressures of NO_2. Any metal center that is present in the surface of the powder and has a relatively small coordination number (or low oxidation state) eventually will get oxidized or nitrated.

III.4. Bonding of NO_2 to $TiO_{2-x}(110)$. To model a TiO_2-(110) surface with O vacancies, we used a four-layer periodic slab with atoms missing from the bridging oxygen rows in the first layer (center of Figure 4).[22,25a] This is the most common position observed for O vacancies when their number is moderate or low.[13,21] In many situations it is unlikely that O vacancies in TiO_2 will assume a periodic array such as that shown in Figure 4, but our model represents well the electronic perturbations associated with the formation of O vacancies (see below). As in the case of the perfect $TiO_2(110)$ slab, the structural geometry of the first two layers in the $TiO_{2-x}(110)$ slab was relaxed while the bottom two layers were kept fixed in the geometry of bulk titania. There was a substantial relaxation in the region near a missing oxygen with the adjacent Ti atoms moving downward and sideways (0.16−0.19 Å) to strengthen their bonds with the remaining oxygens. Figure 9 displays the calculated (DF-GGA) density of states for the occupied bands in the perfect $TiO_2(110)$ slab (bottom panel) and in the $TiO_{2-x}(110)$ slab with O vacancies in the surface

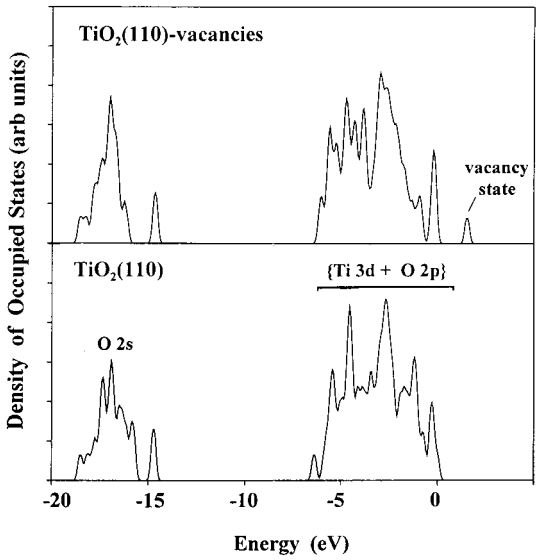

Figure 9. Density functional results for the density of states (DOS) of the occupied bands in $TiO_2(110)$ and a $TiO_{2-x}(110)$ system with O vacancies in the surface. The zero of energy in the figure is not the vacuum level.[24]

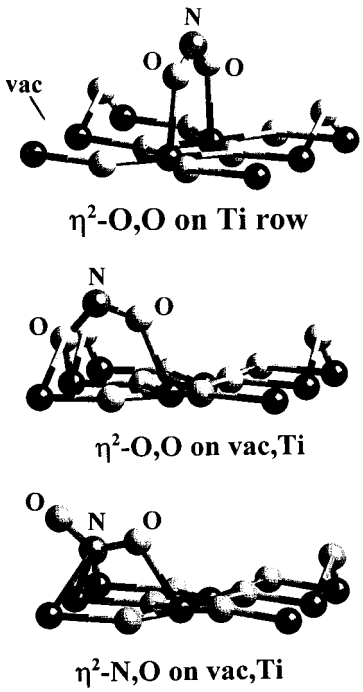

Figure 10. Bonding conformations for NO_2 on a $TiO_{2-x}(110)$ system with O vacancies in the surface. Ti atoms are represented by dark spheres, whereas gray spheres correspond to O atoms.

(46) (a) Derry, D. J.; Lees, D. G.; Calvert, J. M. *J. Phys. Chem. Solids* **1981**, *42*, 57. (b) Sasaki, J.; Peterson, N. L.; Hoshino, K. *J. Phys. Chem. Solids* **1985**, *46*, 1267.

(47) *Lange's Handbook of Chemistry*, 13th ed.; Dean, J. A., Ed.; McGraw-Hill: New York, 1985; pp 9−63.

Table 2. Adsorption of NO_2 on TiO_{2-x}(110): DF-GGA Results

	bond lengths (Å)			NO_2 charge, q (electrons)	ads energy (kcal/mol)[a]
	Ti−N	Ti−O	N−O		
free NO_2			1.21		
on Ti row[b]					
η^2-O,O on Ti,Ti		2.23	1.27	−0.24	24.9
on vacancy sites[b]					
η^2-O,O on vac,Ti		2.17 (2.25)[c]	1.38 (1.25)[c]	−0.46	43.8
η^2-N,O on vac,Ti	2.18	2.20	1.26 (1.30)[c]	−0.49	35.7

[a] Positive values denote an exothermic process.[22,26] [b] $\theta_{NO_2} = 0.25$ ML. [c] The numbers in parentheses are for the O bonded to the Ti rows (see Figure 10).

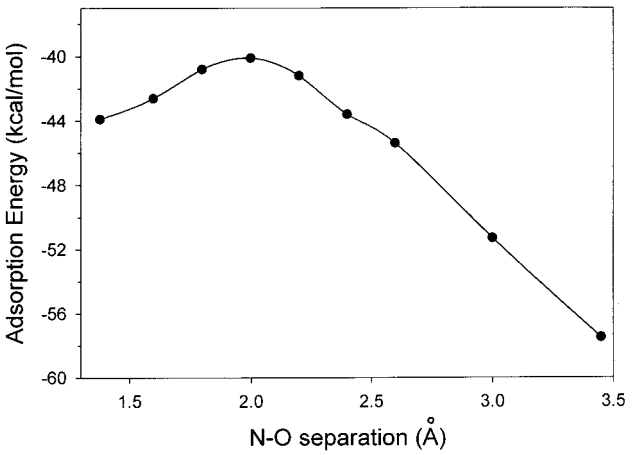

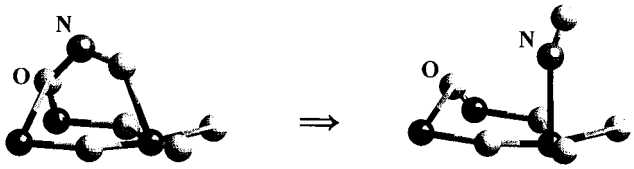

Figure 11. Energy path for the dissociative adsorption of NO_2 on a TiO_{2-x}(110) system with surface vacancies. The precursor for dissociation involves an η^2-O,O coordination of NO_2 above an O vacancy and an atom in a Ti row. In the final state, the O vacancy has been eliminated, and a NO molecule is bonded to an atom in a Ti row via its N end. Ti atoms are represented by dark spheres, whereas gray spheres correspond to O atoms.

(top panel). The valence band in TiO_2(110) contains states of O 2p and Ti 3d character. Since the Ti−O bonds are not fully ionic and have a large degree of covalent character,[22,38a,38b] TiO_2 is best described as an ionocovalent oxide.[38b] The introduction of O vacancies in the TiO_2(110) surface generates a new occupied state that appears ~1.6 eV above the top of the {O 2p + Ti 3d} band and has Ti 3d character. This state is observed in experiments of valence photoemission[13,48] and is frequently attributed to Ti^{3+} ions.[48] Our DF calculations indicate that this vacancy state in TiO_{2-x}(110) plays a predominant role in the bonding and surface chemistry of NO_2.

The NO_2 was bonded to the TiO_{2-x}(110) surface in the configurations shown in Figure 10. They involve coordination to two atoms in a Ti row (η^2-O,O on Ti row), or direct bonding on O vacancies via one O (η^2-O,O on vac,Ti) or N (η^2-N,O on vac,Ti) of the molecule. Table 2 lists structural parameters and adsorption energies obtained after relaxing the geometry of the

(48) Sadeghi, H. R.; Henrich, V. E. *J. Catal.* **1988**, *109*, 1 and references therein.

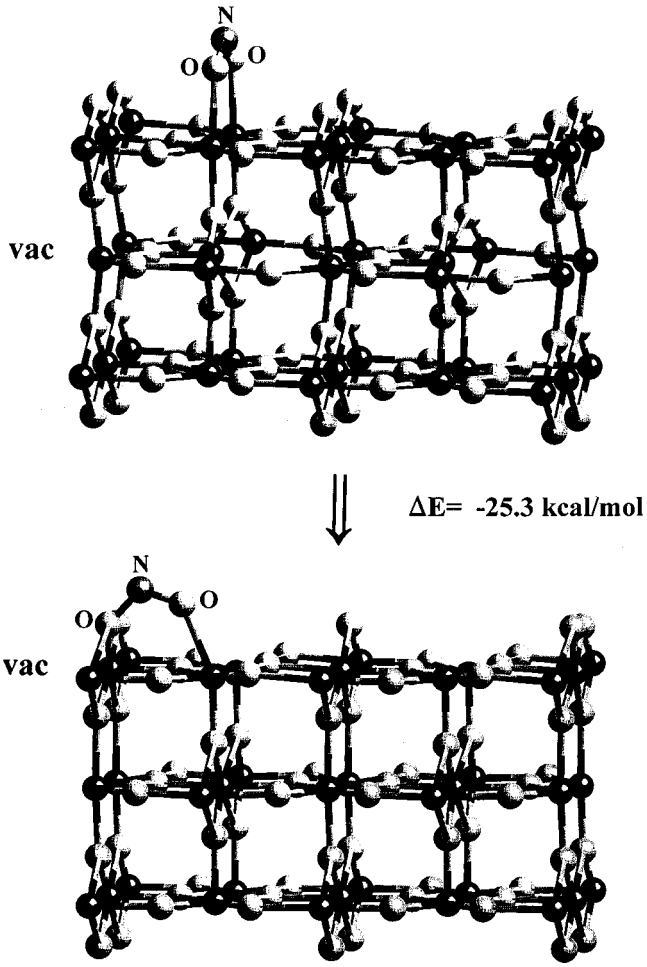

Figure 12. NO_2-induced migration of O vacancies. Initially, NO_2 is adsorbed on the Ti rows and O vacancies are located in the subsurface or bulk region. In the final state, the O vacancies have moved to the surface and half of them are "covered" by O atoms of NO_2. In the scheme, only three of the four layers in the slab models are shown. Ti atoms are represented by dark spheres, whereas gray spheres correspond to O atoms.

adsorbate ($\theta_{NO_2} = 0.25$ ML) and first two layers in our slab model. In the presence of O vacancies, the bonding energy of NO_2 on two atoms of a Ti row (24.9 kcal/mol) is larger than that found on a perfect TiO_2(110) surface (21.3 kcal/mol), but not as large as those seen for adsorption of the molecule above O vacancies (36−44 kcal/mol). In these adsorption sites, the underlying Ti atoms interact very well with the LUMO of the NO_2 molecule ($6a_1$ orbital[7,43]), with a substantial Ti(3d) → NO_2-($6a_1$) electron transfer and a weakening of the N−O bonds that facilitates dissociation of the adsorbate.

The most stable bonding configuration in Figure 10 corresponds to NO_2 adsorbed with one of its O atoms above an oxygen vacancy and the other O near an atom in a Ti row. This configuration is characterized by one very large N−O bond distance (1.38 Å) and is an ideal precursor for dissociation of the NO_2 molecule. Figure 11 shows calculated energy changes along a possible reaction path for the

$$NO_2(ads) \rightarrow NO(ads) + O(ads) \qquad (6)$$

reaction on a TiO_{2-x}(110) surface. In the final state, the produced NO fragment is adsorbed on a Ti row, and an O vacancy has been eliminated. To obtain the curve in Figure 11, for each N−O separation, we relaxed all the other structural parameters of the

surface. Overall, the NO_2 dissociation process on an O vacancy is exothermic ($\Delta E = -13.6$ kcal/mol), with a small activation energy barrier (3.8 kcal/mol). The same reaction on the Ti rows of a perfect $TiO_2(110)$ surface is an endothermic process ($\Delta E = +4.3$ kcal/mol). If the concentration of O vacancies in the oxide surface is large, the NO produced by reaction 6 could be decomposed into atomic N and O. If no O vacancies are present, the NO, which is weakly bound to the Ti sites (see above), could desorb at temperatures below 300 K or be displaced by an NO_2 molecule. The DF calculations indicate that reactions 2 and 6 are the key to the chemistry of NO_2 on $TiO_2(110)$. First, reaction 6 eliminates O vacancies from the oxide surface. This is then followed by the formation of NO_3 on the Ti rows by reaction 2.

The photoemission experiments in section III.1 show that NO_2 can oxidize Ti^{3+} sites located in the subsurface or bulk regions of titania. Our DF results indicate that this phenomenon reflects changes induced by NO_2 on the relative stability of O vacancies in the surface versus subsurface regions. After cleaning/preparing a titania sample, one obtains a distribution of O vacancies from the surface to the bulk of the system.[13,21,46] Using the two slab models shown at the center and bottom of Figure 4, we compared the thermochemical stability of O vacancies in the surface and subsurface regions of $TiO_2(110)$. After structural relaxation of the top two layers in each slab, the DF-GGA calculations give a small difference in stability (<3 kcal/mol) that is within the accuracy of the theoretical method.[25a,33] On the other hand, when NO_2 is present on the surface, the migration of O vacancies from the subsurface region to the surface (see Figure 12) is a highly exothermic process ($\Delta E = -25.3$ kcal/mol). *Such migration is a requirement for the dissociation of adsorbed NO_2*, and eventually leads to oxidation or elimination of Ti^{3+} centers. Furthermore, DF calculations indicate that adsorbed NO and N_2O also facilitate the movement of oxygen vacancies from the bulk to the surface of titania from a thermochemical viewpoint. In the case of N_2O adsorption, we have verified this prediction in experiments similar to those seen in Figure 7. Thus, in DeNOx operations, not only the surface properties of an oxide are important. In addition, the subsurface composition of the sorbent/catalyst can determine the trapping of NO_x species and N−O bond cleavage.

IV. Conclusions

The main product of the adsorption of NO_2 on $TiO_2(110)$ is surface nitrate with a small amount of chemisorbed NO_2. A similar result is obtained after the reaction of NO_2 with polycrystalline powders of TiO_2 or other oxides (MgO, CeO_2, Cr_2O_3, Fe_2O_3, CuO, ZnO). This trend, however, does not imply that the metal centers of the oxides are unreactive toward NO_2. Photoemission data and DF calculations indicate that the surface nitrate forms through the disproportionation of NO_2 on Ti sites ($2NO_{2,ads} \rightarrow NO_{3,ads} + NO_{gas}$) rather than direct adsorption of NO_2 on O centers of titania. $Ti^{\delta+}$ ($\delta \leq 3$) centers present on $TiO_{2-x}(110)$ surfaces react readily with NO_2 and eventually all become oxidized or covered with nitrate. The interactions between NO_2 and O vacancies of $TiO_2(110)$ are complex. Electronic states associated with O vacancies interact very well with the LUMO of NO_2, with a substantial $Ti(3d) \rightarrow NO_2(6a_1)$ electron transfer and a weakening of the N−O bonds that favors dissociation of the molecule. This changes the chemistry of NO_2 on $TiO_2(110)$. At the same time, the adsorbed NO_2 affects the thermochemical stability of O vacancies, facilitating their migration from the bulk to the surface of titania. The behavior of the NO_2/titania system illustrates the importance of surface *and* subsurface defects when dealing with DeNOx reactions on oxides.

Acknowledgment. The authors thank S. Sambasivan and D. Fischer for their help with the use of the XANES instrumentation at beamline U7A of the NSLS. This research was carried out at Brookhaven National Laboratory under contract DE-AC02-98CH10086 with the U.S. Department of Energy (Division of Chemical Sciences). The NSLS is supported by the Divisions of Materials and Chemical Sciences of DOE.

JA011131I